

# Fourier Transform Infrared and $^{13}\text{C}$ -NMR Spectroscopic Characterization of Model Epoxy Networks

F. GALLOUEDEC, F. COSTA-TORRO, F. LAUPRETRE, and B. JASSE\*

Laboratoire de Physicochimie Structurale et Macromoléculaire, Ecole Supérieure de Physique et Chimie Industrielles, 10 rue Vauquelin, 75231 Paris Cedex 05, France

## SYNOPSIS

Model epoxy networks based on a diglycidylether of bisphenol A (DGEBA) or of butanediol (DGEBU) and cured with different mixtures of monoamines and diamines were prepared to allow changes in cross-link density. The choice of aliphatic or aromatic amines permitted assessment of the influence of network chain flexibility. Solid state  $^{13}\text{C}$ -NMR spectra showed that no secondary reactions leading to the creation of ether linkage occur during the condensation reaction. Glass transition temperatures ( $T_g$ ) and the temperatures of the maximum of the exothermic cross-linking reaction ( $T_{exo}$ ) were determined. A rectilinear increase of  $T_g$  as a function of the density of cross-links was observed for all the systems under study. Similarly, an increase in the stiffness of the backbone units resulted in an increase in  $T_g$ . Time-temperature-transformation (TTT) isothermal cure diagrams were constructed and infrared kinetics were performed at 90°C. Gelation and vitrification times were shown to be dependent on the nature of the amines used to create the network structure. © 1993 John Wiley & Sons, Inc.

## INTRODUCTION

In the last decade, numerous studies have been devoted to the determination of the relationships existing between the chemical structure and the properties of various epoxy networks that are to be used as matrices for composite materials. However, such studies usually deal with commercial networks whose chemical reactions and network structures are not well defined. For the purpose of separating the influences of the cross-link density and chain flexibility on the properties of epoxy networks, we prepared "model" networks based on a diglycidyl ether of bisphenol A (DGEBA) or of butanediol (DGEBU) cured with different mixtures of monoamines and diamines to allow changes in cross-link density. The choice of different types of amines (aliphatic or aromatic) permitted assessment of the influence of network chain flexibility. This was also achieved by replacing DGEBA by DGEBU. Using a pure diamine, a mixture of diamine/monoamine or a pure monoamine leads to a network structure going progressively from a highly cross-linked resin

to a linear polymer, as illustrated in Figure 1 for the DGEBA/HA/HMDA resins. The viscoelastic properties of some of these model networks have already been published<sup>1</sup> and the present paper is devoted to their characterization.

## EXPERIMENTAL

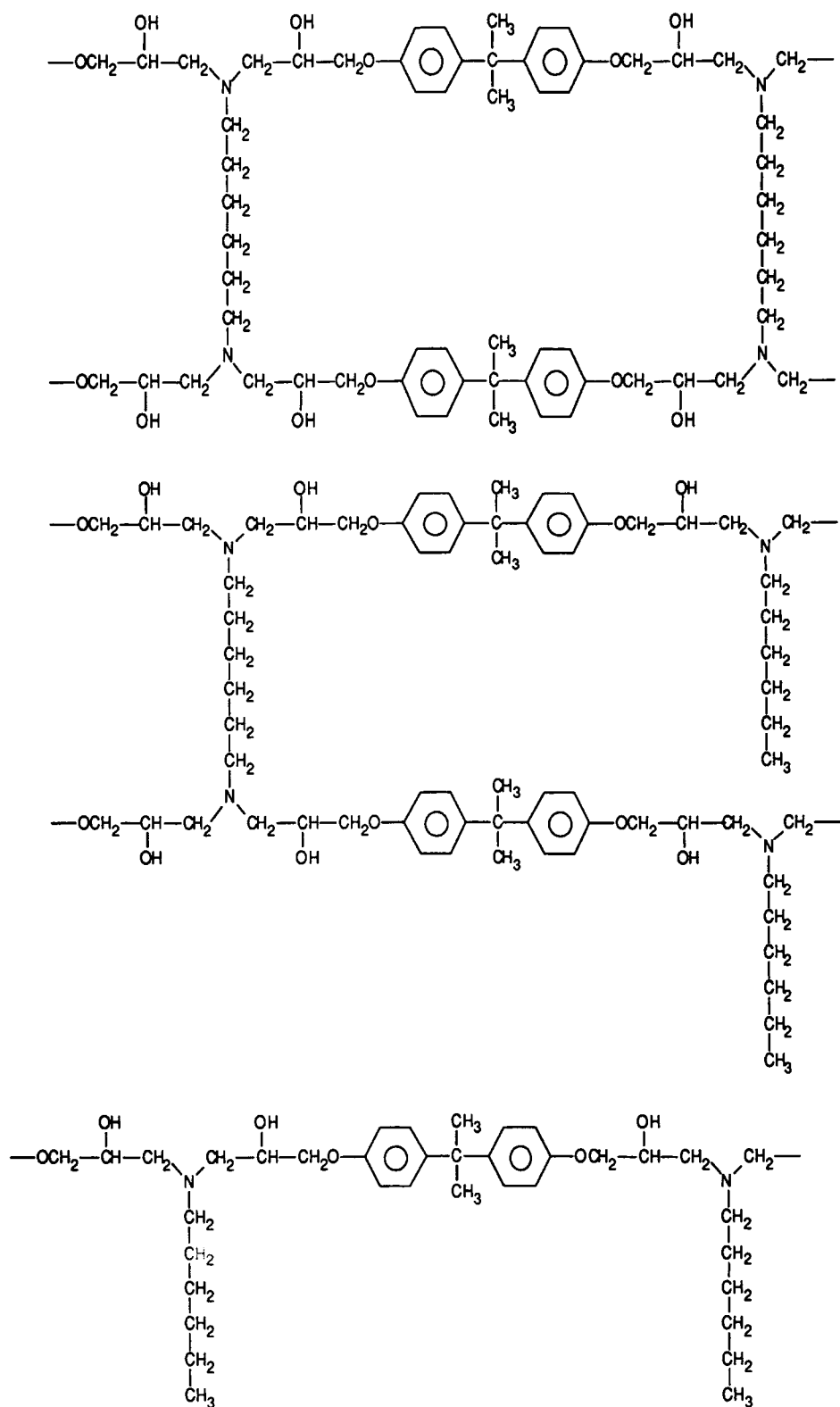
### Materials

Characteristics and origins of the chemicals used in this study are summarized in Table I. The two diepoxydes were of high purity and of a very low degree of polymerization  $n$  ( $n \leq 0.03$ ). All the amines under study were of high purity grade.

### Sample Preparation

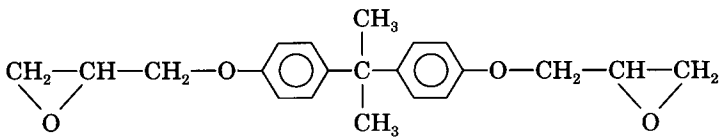
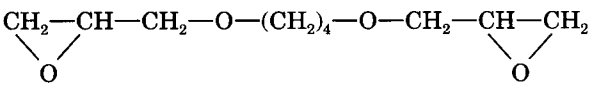
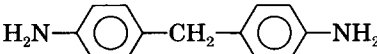
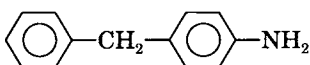
In all the systems under study, the stoichiometric ratio of epoxy to the NH ratio was maintained to unity. The amines were added to the epoxy prepolymer under nitrogen at the lowest temperature for which a complete dissolution occurs without any noticeable chemical reaction. The dissolution temperature depends on the amine melting point and on the epoxy and amine reactivity (it ranges from

\* To whom correspondence should be addressed.



**Figure 1** Schematic representation of the different networks for DGEBA/HA/HMDA resins.

**Table I Epoxy Prepolymers and Amines Used for the Synthesis of Epoxy Networks**

Product	Formula	Supplier
DGEBA		Bakelite Rutapox 0162
DGEBU		Ciba DY026SP
HMDA	$\text{H}_2\text{N}-(\text{CH}_2)_6-\text{NH}_2$	Merck
HA	$\text{CH}_3-(\text{CH}_2)_5-\text{NH}_2$	Merck
DDM		Fluka
ADM		ONERA

room temperature for DGEBU/amine up to 80°C for DGEBA/DDM).

Cured resins were obtained by heating the epoxy-monoamine-diamine resins under a nitrogen atmosphere for 20 h at the exotherm temperature. Epoxy-diamine systems were then postcured for 24 h at 60°C above the exotherm temperature. Cured resins thus obtained were investigated by high-resolution solid-state  $^{13}\text{C}$ -NMR, FTIR, and DSC. Their glass-transition temperatures show no further increase with increasing postcure duration.

### Thermal Analysis

The thermograms were obtained using a DuPont 1090 differential scanning calorimeter at a heating rate of 10°C min<sup>-1</sup>; sample weight was 5–10 mg.  $T_g$  was measured in the DSC curve as the point of intersection of the extrapolated base line at the low-temperature end and the tangent to the curve at the inflection point.

### Infrared Measurements

Infrared spectra were obtained on a Nicolet 7199 Fourier transform infrared spectrometer. Thirty-two co-added interferograms were scanned at 2 cm<sup>-1</sup> resolution. For kinetics studies, we used a Mettler FP 82 heating cell directly located in the sample compartment of the spectrometer with the sample placed between two KBr plates. The cell was pre-

heated at the reaction temperature and the initial reaction time was arbitrarily chosen as the time of introduction of the sample. Isothermal heating was monitored at  $\pm 0.2^\circ\text{C}$ .

### $^{13}\text{C}$ -NMR Measurements

High-resolution solid-state  $^{13}\text{C}$ -NMR measurements were obtained by using the combined techniques of cross-polarization, proton dipolar decoupling, and magic-angle spinning<sup>2</sup> at the operating frequency of 25.15 MHz on a Bruker CXP-100 spectrometer. The matched spin-lock cross-polarization transfers used  $^{13}\text{C}$  and  $^1\text{H}$  magnetic field strengths of 60 kHz. Contact durations were 1 ms. The spinning speed was of the order of 3.5 kHz. Spin-inversion techniques were used to minimize base-line noise and roll.<sup>3</sup> Flip-back<sup>4</sup> was also used to shorten the delay time between two successive pulse sequences.

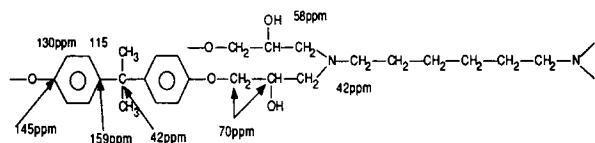
### Torsional Braid Analysis (TBA)

Specimens were prepared using multifilamental carbon braids (length = 50 mm; diameter = 2 mm) impregnated with the epoxy/amine mixture. Data were obtained from a Torsiomatic Zwick 5203 pendulum at a frequency of 10 Hz. The times to gelation and vitrification were assigned from the maxima of the logarithmic decrement vs. the isothermal cure time plots and used to construct an isothermal time-temperature-transformation (TTT) cure diagram.

## RESULTS AND DISCUSSION

### Characterization of the Chemical Structure of Cured Epoxy–Amine Systems

There is a number of reactions that can occur during the curing of epoxy–amine resins. Among them, under usual cure conditions, the dominant reactions are the addition of a primary amine function onto an epoxy group, leading to a secondary amine and hydroxyl group, and the addition of the secondary amine thus obtained onto another epoxy group, leading to a tertiary amine.<sup>5</sup> Other reactions may involve the addition of the secondary alcohol functions formed in the previous main reactions onto the epoxy functions and homopolymerization of epoxy functions. They are characterized by the formation of ether groups.<sup>6</sup> The 25 MHz high-resolution solid-state  $^{13}\text{C}$ -NMR spectra of the cured resins based on DGEBA and HA/HMDA mixtures are shown in Figure 2. The line assignment is based on the  $^{13}\text{C}$ -NMR chemical shifts of the starting materials and compounds obtained from model reactions.<sup>7,8</sup> As an example, the NMR peak assignment of the DGEBA–HMDA system is summarized below:



In the whole series of spectra, the peak in the 70 ppm region can be assigned to  $-\text{CH}_2-\text{CHOH}-$  carbons resulting from the dominant epoxy–amine addition. The 58 ppm line corresponds to  $\text{CH}_2$  groups next to cross-links. On the other hand, the existence of ether groups, formed from secondary reactions and corresponding to  $-\text{CH}-\text{O}-$  carbons resonating in the neighborhood of 77 ppm,<sup>7,8</sup> cannot be detected in the spectra, at the sensitivity of the experiments. Moreover, the absence of a 45 ppm line indicates that there is no residual epoxy groups at the sensitivity of the experiments. This last point is supported by the absence of the  $915\text{ cm}^{-1}$  band in the FTIR spectrum characteristic of the absorption of epoxy groups. Therefore, observations based on both FTIR and high-resolution solid-state  $^{13}\text{C}$ -NMR spectra show that the cured resins based on DGEBA and HA/HMDA mixtures are largely formed by epoxy–amine additions, without detectable residual epoxy groups and ether functions formed by secondary reactions. The latter result is in agreement

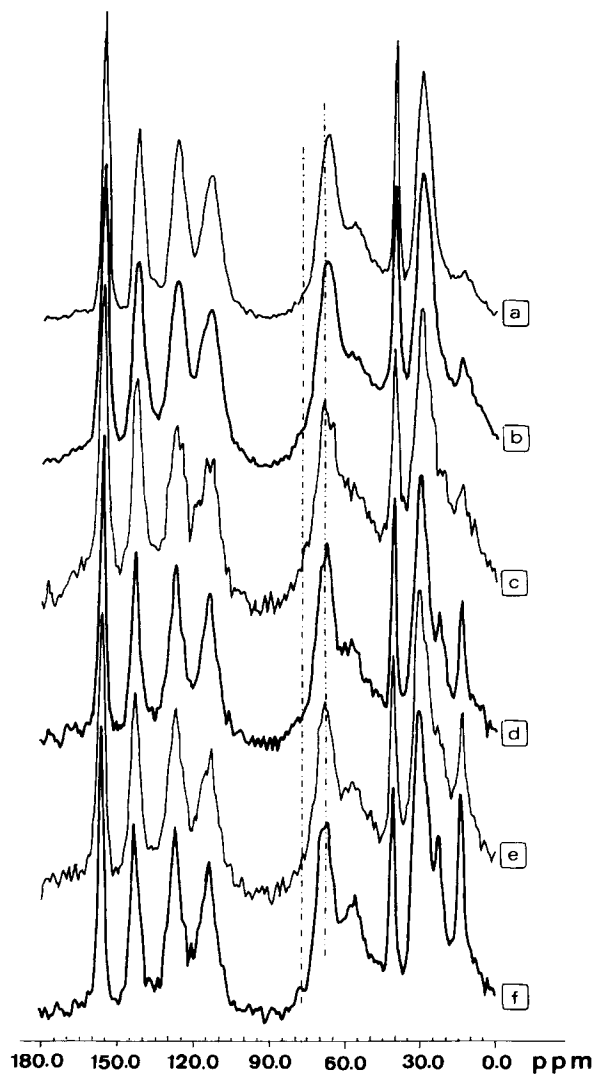


**Figure 2** High-resolution solid-state  $^{13}\text{C}$ -NMR spectra of DGEBA/HA/HMDA-cured resins: (a) 0% HA; (b) 20% HA; (c) 40% HA; (d) 60% HA; (e) 80% HA; (f) 100% HA.

with the conclusions of several papers<sup>9–13</sup> that have shown that under similar cure conditions (stoichiometric proportions, curing temperature equal to or slightly above the exotherm temperature, and absence of a catalyst) the side reactions during the DGEBA–amine cure were neglectable. Similar conclusions have been derived for all the systems under study. Therefore, the resins under study have a chemical structure as simple as possible and, as such, they may be considered as “model networks.”

### Thermal Analysis

Thermal analysis allows one to point out the temperature of the maximum of the exothermic cross-

linking reaction,  $T_{\text{exo}}$ , and to determine the glass transition temperature,  $T_g$ , of highly cured resins. The results are given in Table II for DGEBA/amine resins and in Table III for DGEBU/amine resins. These results show that the temperature of the exotherm,  $T_{\text{exo}}$ , decreases regularly with an increase of the diamine amount in the resin when the mono- and the diamine have the same chemical character (aliphatic or aromatic). On the other hand, when these structures are different, two exotherms are observed on account of the greater reactivity of aliphatic amines with respect to the aromatic amines. The intensity of the two exotherms is directly related to the relative amount of the two amines in the resin.

The changes of glass transition temperature of cross-linked resins as a function of the amount of diamine in the resins do not follow a linear relationship but for two resins: DGEBA/HA/HMDA and DGEBU/ADM/DDM. To compare the different resins in terms of stiffness, it is necessary to compare the results at the same density of cross-links per volume unit. For a diepoxy/diamine resin,

**Table II**  $T_{\text{exo}}$  and  $T_g$  for DGEBA-based Resins

Monoamine (%)	Diamine (%)	$T_{\text{exo}}$ (°C)	$T_g$ (°C)
<u>HA</u>	<u>HMDA</u>		
100	0	113	42
80	20	108	50
60	40	109	63
40	60	107	81
20	80	102	93
0	100	102	107
<u>ADM</u>	<u>DDM</u>		
100	0	184	90
75	25	180	97
50	50	174	115
25	75	172	138
0	100	168	179
<u>HA</u>	<u>DDM</u>		
100	0	113	42
75	25	114–165 (shoulder)	68
50	50	115–168	98
25	75	115 (shoulder)–168	136
0	100	168	179
<u>ADM</u>	<u>HMDA</u>		
100	0	184	90
75	25	106–175 (shoulder)	90
50	50	116–173	91
25	75	110 (shoulder)–176	100
0	100	102	107

**Table III**  $T_{\text{exo}}$  and  $T_g$  for DGEBU-based resins

Monoamine (%)	Diamine (%)	$T_{\text{exo}}$ (°C)	$T_g$ (°C)
<u>HA</u>	<u>HMDA</u>		
100	0	138	–48
75	25		–42
50	50	121	–35
25	75		–28
0	100	114	–12
<u>ADM</u>	<u>DDM</u>		
100	0	190	9
75	25		20
50	50	180	38
25	75		49
0	100	169	66

it can be shown<sup>14</sup> that the number  $N$  of diamine moiety per volume unit is given by the relation

$$N \text{ (mol dm}^{-3}\text{)} = \frac{1000\rho Nd}{NeMe + NdMd}$$

where  $\rho$  is the density of the resin;  $Ne$  and  $Nd$ , the number of moles; and  $Me$  and  $Md$ , the molecular weights of the epoxy and diamine, respectively.

When a monoamine is added in the resin,  $N$  is given by

$$N \text{ (mol dm}^{-3}\text{)} = \frac{1000\rho Nd}{NeMe + NdMd + NmMm}$$

where  $Nm$  and  $Mm$  are the number of moles and molecular weight of the monoamine, respectively.

Using the values of  $\rho$  given in Ref. 14, we obtained the results shown in Figures 3 and 4 for the change of  $T_g$  as a function of  $N$ . A rectilinear behavior is observed for all the systems under study.

As expected, an increase of the diamine percentage that increases the number of cross-links results in an increase of  $T_g$ . Similarly, an increase in the stiffness of the backbone units (aromatic structures) results in an increase in  $T_g$ .

## Characterization of the Network Construction

### Torsional Braid Analysis

The time–temperature–transformation (TTT) diagram is an interesting way to represent the different stages that are encountered in the cure of epoxy sys-

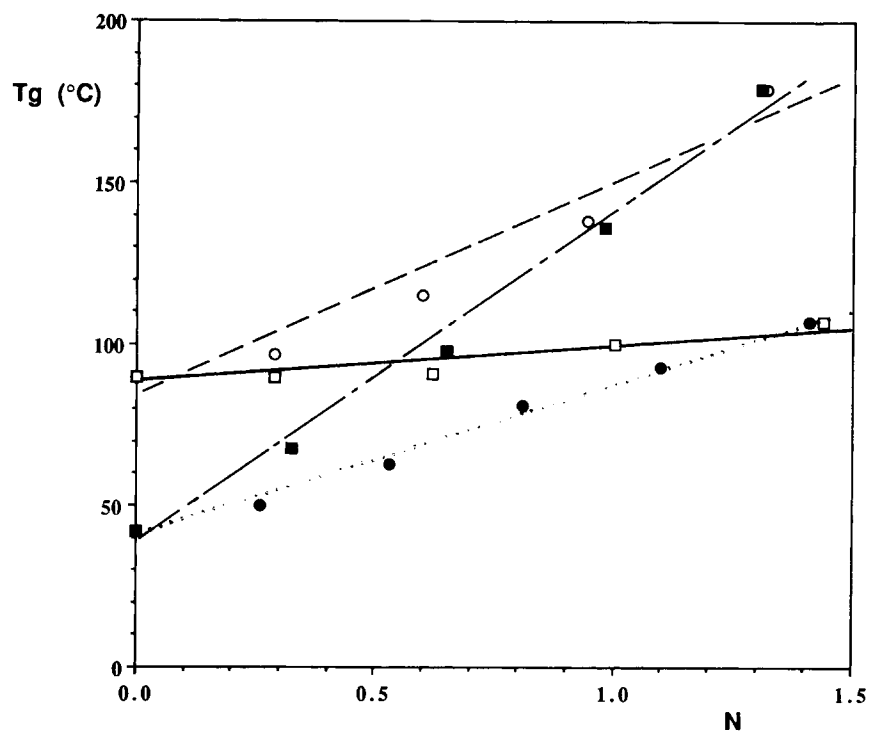


**Figure 3** Glass transition temperatures of DGEBA-based resins as a function of the density of cross-links,  $N$ : (●) DGEBA/HA/HMDA; (□) DGEBA/ADM/HMDA; (○) DGEBA/ADM/DDM; (■) DGEBA/HA/DDM.

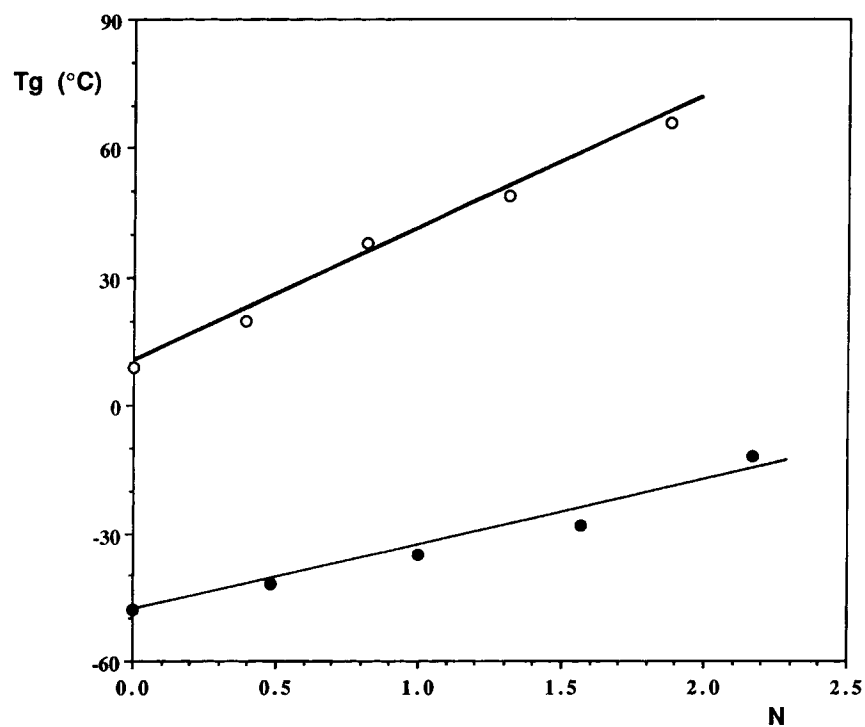


**Figure 4** Glass transition temperatures of DGEBU-based resins as a function of the density of cross-links,  $N$ : (●) DGEBU/HA/HMDA; (○) DGEBU/ADM/DDM.

tems vs. the isothermal temperature of cure.<sup>15</sup> Two important times of reaction can be identified in the diagram:  $t_{\text{gel}}$  and  $t_v$ , at a given temperature. The time  $t_{\text{gel}}$  is defined as the time at which gelation of the material occurs, whereas  $t_v$  corresponds to the reaction time necessary to reach vitrification. Furthermore, two characteristic temperatures can be deduced from the TTT cure diagrams: gel  $T_g$  and  $T_{g\infty}$ . Gel  $T_g$  is defined as the glass transition temperature of the material at gelation and corresponds approximately to the isothermal cure temperature at which gelation and vitrification coincide.  $T_{g\infty}$  is the maximum glass transition temperature obtained by isothermal cure.

In the present work, we limited our study to the influence of chain stiffness and/or cross-link density on the properties of model networks that exhibit a similar glass transition temperature. From the DSC results, we chose different DGEBA/amine systems that have a glass transition temperature close to 90°C after curing. Table IV sums up the composition and  $T_g$  values of the four resins studied. The corresponding TTT diagrams are shown in Figure 5. It can be noticed that the  $T_{g\infty}$  values obtained from the diagrams are higher than the values obtained from DSC, a  $\Delta T_g$  between 20 to 40°C being observed. Such an effect can be assigned to (i) the change of frequency of measurement between DSC ( $\sim 1$  Hz) and TBA (10 Hz); (ii) the use of the logarithmic decrement to determine vitrification, which is known to reflect the last steps of the vitrification processes and thus to introduce a  $\Delta T_g$  of about 30°C in epoxy resins.<sup>16</sup>

The influence of the reactivity of the mono- and diamines is well illustrated by the diagrams. As a matter of fact, gelation is related to the appearance of an infinite macromolecular weight  $M_\infty$  that is directly dependent on the diamine amount in the epoxy resin. Gelation occurs at a shorter time scale when an aliphatic diamine (HMDA) is present in

the resin, according to the higher reactivity of aliphatic amines with epoxy groups. When an aromatic diamine (DDM) is used as the cross-linking agent, gelation occurs at a longer time scale. On the other hand, vitrification takes place at a longer time scale when an aromatic monoamine (ADM) is present in the HMDA resin. When an aromatic diamine (DDM) is used as the cross-linking agent, gelation occurs at a long time scale and no further significant influence of the aliphatic or aromatic character of the monoamine on vitrification can be observed. These points will be discussed in more detail in the next section.

### Fourier Transform Infrared Analysis

Fourier transform infrared (FTIR) analysis of epoxy/amine resins allows one to follow the change of reactive species as a function of curing time. We studied the reaction kinetics of the four resins used in the previous section in order to have a deeper insight of the chemical processes involved in the gelation and vitrification curves obtained in the TTT diagrams.

To obtain comparative results between the different sets of measurements, it is necessary to use an internal thickness band to normalize the spectra. Two different absorption bands were used for this purpose depending on the DGEBA/amine resins. In the HA/DDM and HA/HMDA resins, the 1605  $\text{cm}^{-1}$  phenyl group absorption band of DGEBA was chosen for the normalization. On the other hand, in the DDM/ADM and HMDA/ADM resins, the 700  $\text{cm}^{-1}$  phenyl group absorption band was preferred to the 1605  $\text{cm}^{-1}$  band, which is too strong and does not obey Beer's law any more.

Although absorption bands of the different components badly overlap in the spectra of the resins, some of the chemical functions involved in the curing reaction can be detected, i.e., epoxy, primary amine, and hydroxyl groups.

An isolated absorption band corresponding to an epoxide deformation vibration<sup>17</sup> is observed at 915  $\text{cm}^{-1}$  in the DGEBA/amine spectrum. Primary amine stretching absorptions usually appear in the following ranges: dialkyl 3398–3381  $\text{cm}^{-1}$ , 3344–3324  $\text{cm}^{-1}$ , diaryl 3509–3460  $\text{cm}^{-1}$ , and 3416–3382  $\text{cm}^{-1}$ . All these absorption bands move to lower frequencies on association.<sup>18</sup> In the HMDA/ADM and HA/DDM resins, amine bands are observed at 3375 and 3460  $\text{cm}^{-1}$ . We chose the 3375  $\text{cm}^{-1}$  band to follow the reaction. This absorption band is too strong in the DDM/ADM resin, so we preferred the 3460  $\text{cm}^{-1}$

**Table IV** Composition and  $T_g$  Values (DSC) of DGEBA/Amine Resins Used in the Torsional Braid and FTIR Analysis

Monoamine (%)	Diamine (%)	$T_g$ (°C)
HA 22.5	HMDA 77.5	86
ADM 40	HMDA 60	92
HA 53.5	DDM 46.5	85
ADM 87.5	DDM 12.5	91

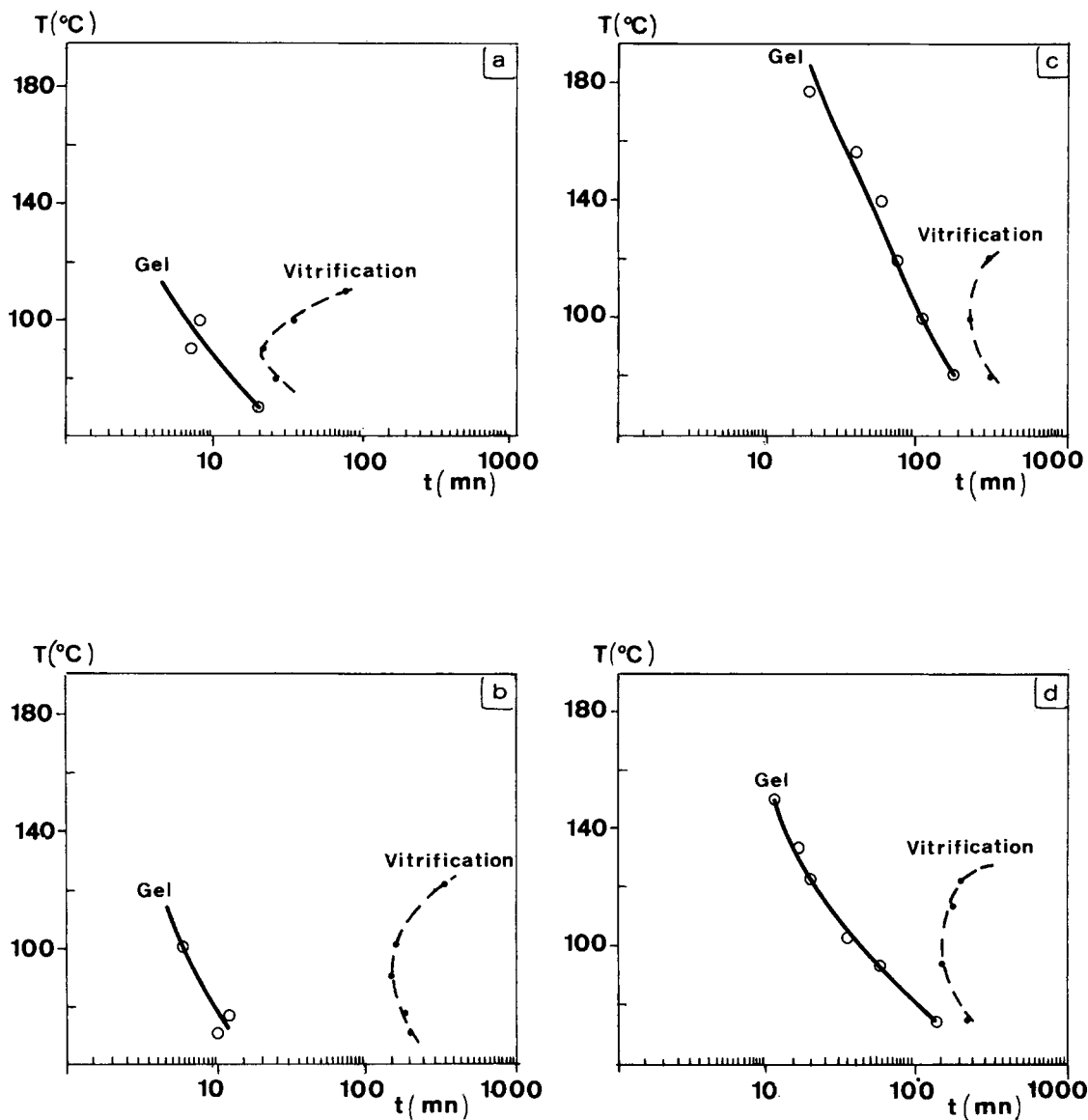


**Figure 5** The TTT cure diagrams for the DGEBA-based resins: (a) DGEBA/HA/HMDA; (b) DGEBA/ADM/HMDA; (c) DGEBA/ADM/DDM; (d) DGEBA/HA/DDM.

band for this system. In HA/HMDA resins, no information on the amine group disappearance can be obtained since amine bands are not detectable. Aliphatic  $\text{NH}_2$  functions react very quickly and have disappeared completely at the start of the FTIR measurements. The  $\beta_s$  ( $\text{NH}_2$ ) vibrational mode that is observed in the range  $1620\text{--}1630\text{ cm}^{-1}$  badly overlaps a phenyl mode observed at  $1605\text{ cm}^{-1}$  in DGEBA and appears as a shoulder not usable for quantitative determinations.

As soon as the curing reaction starts, hydroxyl and secondary amine functions are generated. OH

group vibrations appear as a broad absorption band around  $3550\text{ cm}^{-1}$  (OH stretching) and  $1107\text{ cm}^{-1}$  (OH deformation). The amount of secondary amine cannot be determined quantitatively. However, it is very difficult to avoid any reaction between DGEBA and primary amine functions when the resins are prepared and a relative amount of secondary amine groups is always present when the first infrared spectrum is scanned.

The infrared kinetics were performed at  $90^\circ\text{C}$ , a temperature that is close to the  $T_g$ 's (DSC) of the four resins. This temperature was chosen in order



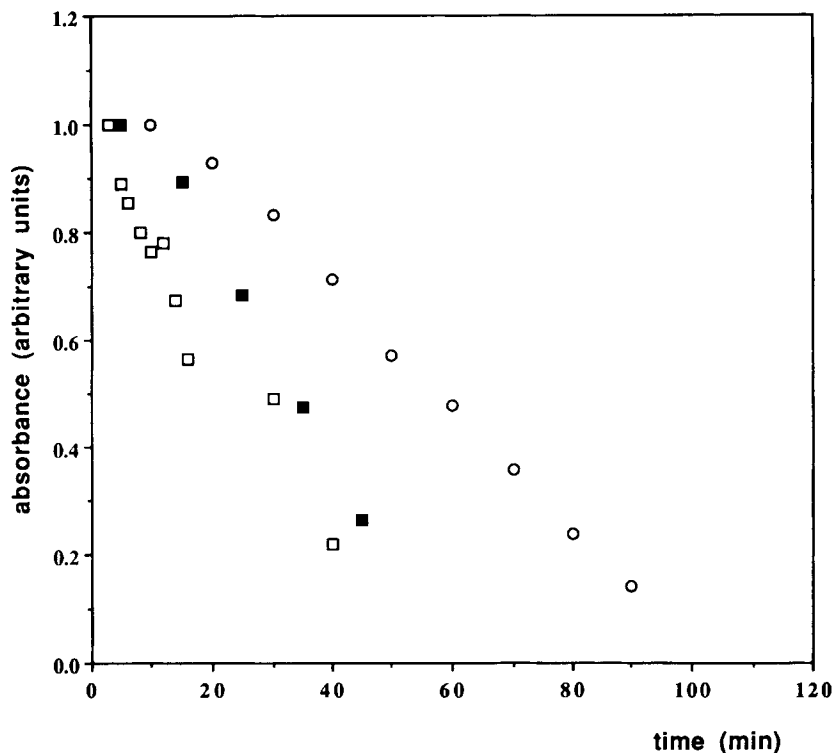


**Figure 6**  $\text{NH}_2$  groups as a function of curing time: (□) DGEBA/ADM/HMDA; (○) DGEBA/ADM/DDM; (■) DGEBA/HA/DDM.

to cross the gelation and vitrification curves of the TTT diagrams.

The reaction of  $\text{NH}_2$  groups is shown in Figure 6. The change of epoxy and hydroxyl groups is shown in Figure 7(a)–(d).

Two different cases have to be considered;

- (i) The diamine is aliphatic [Fig. 7(a) and (b)].

In that case, the reaction rate of the diamine is fast, and, as we have previously seen in the TBA analysis, gelation, which is governed by the diamine, occurs at short reaction times. As expected, infrared results indicate that at  $t_{\text{gel}}$  the conversion rate of epoxy groups is not complete. The reaction rate of the epoxy functions is similar in the two systems. After gelation, the completion of the reaction goes on, and when the vitrification is reached, the epoxy groups do not react anymore. The aliphatic or aromatic character of the monoamine does not seem to have any influence except on the vitrification time.

- (ii) The diamine is aromatic [Fig. 7(c) and (d)].

In the DDM/HA resin, the aliphatic monoamine reacts dominantly during the gelation

process, which results in a gelation time  $t_{\text{gel}}$  shorter than the gelation time of the DDM/ADM resin based on aromatic amines [see Fig. 5(c) and (d)]. Gelation occurs when  $\text{NH}_2$  functions have completely disappeared and more or less at the end of reaction of the epoxy groups. Vitrification is undetectable on the kinetic curves, TBA vitrification times being similar in the two systems.

In conclusion, the gelation time, which depends mainly on the extent of reaction of the diamine, is not strongly influenced by the nature of the monoamine when the diamine is aliphatic. A shortening of the gelation time is observed when the diamine is aromatic and the monoamine aliphatic. In the resins that contain an aliphatic diamine, gelation occurs before the end of reaction of the epoxy groups, the effect being more pronounced when the monoamine is aromatic (longer reaction times). The vitrification time is not much influenced by the nature of the diamine ( $150 \text{ min} < t_v < 200 \text{ min}$ ) in the resins that contain an aromatic mono- or diamine, whereas  $t_v$  is considerably shortened ( $t_v = 20 \text{ min}$ ) when the resin is wholly aliphatic.

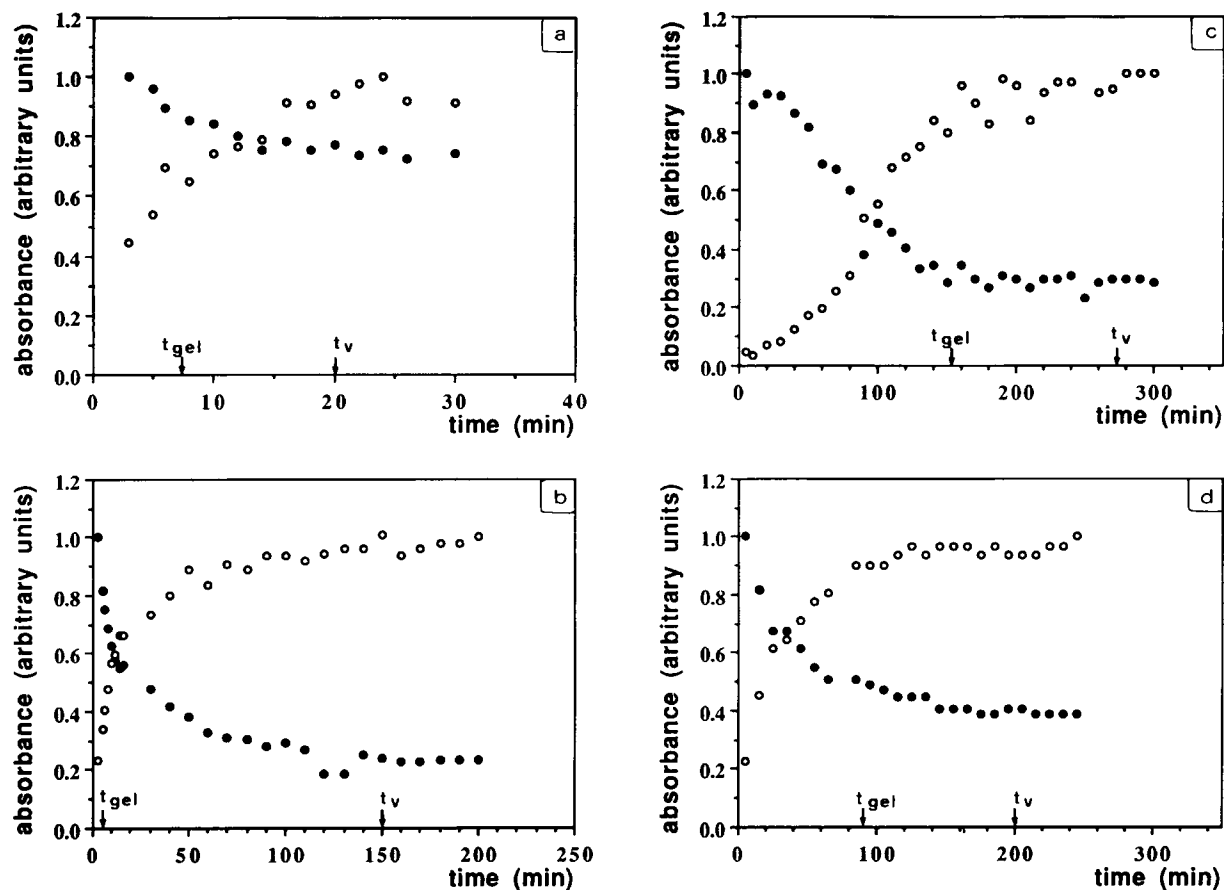


**Figure 7** Epoxy (●) and hydroxyl (○) groups as a function of curing time: (a) DGEBA/HA/HMDA; (b) DGEBA/ADM/HMDA; (c) DGEBA/ADM/DDM; (d) DGEBA/HA/DDM.

## REFERENCES

1. S. Cukierman, J. L. Halary, and L. Monnerie, *J. Non-Cryst. Solids*, **131–133**, 898 (1991).
2. J. Schaefer, E. O. Stejskal, and R. Buchdahl, *Macromolecules*, **10**, 384 (1977).
3. E. O. Stejskal and J. Schaefer, *J. Magn. Reson.*, **18**, 560 (1975).
4. J. Tegenfeldt and U. Haeberlen, *J. Magn. Reson.*, **36**, 453 (1979).
5. C. A. May and Y. Tanaka, *Epoxy Resins, Chemistry and Technology*, Marcel Dekker, New York, 1973.
6. C. C. Riccardi and R. J. J. Williams, *J. Appl. Polym. Sci.*, **32**, 3445 (1986).
7. M. F. Grenier-Loustalot and P. Grenier, *Eur. Polym. J.*, **22**, 457 (1986).
8. A. J. Attias, J. Ancelle, B. Bloch, and F. Lauprêtre, *J. Polym. Sci. Polym. Chem. Ed.*, **28**, 1661 (1990).
9. L. Shechter, J. Wynstra, and R. P. Kurkijy, *Ind. Eng. Chem.*, **48**, 94 (1956).
10. C. A. Byrne, N. S. Schneider, and G. L. Hagnauer, *Proceedings of the IUPAC Macro 82*, Amherst, 1982, p. 686.
11. C. A. Byrne, G. L. Hagnauer, and N. S. Schneider, *Polym. Compos.*, **4**, 213 (1983).
12. T. K. Kwei, *J. Polym. Sci. A1*, 2977 (1963).
13. M. F. Grenier-Loustalot and P. Grenier, *J. Polym. Sci. Polym. Chem. Ed.*, **22**, 4011 (1984).
14. S. Cukierman, Thesis, Paris, 1991.
15. J. K. Gillham, *Development in Polymer Characterisation-3*, J. V. Dawkins, Ed., Applied Science, London, 1982, p. 159.
16. K. P. Pang and J. K. Gillham, *J. Appl. Polym. Sci.*, **37**, 1969 (1989).
17. G. C. Stevens, *J. Appl. Polym. Sci.*, **26**, 4259 (1981).
18. L. J. Bellamy, *The Infrared Spectra of Complex Molecules-1*, Chapman and Hall, London, 1975.

Received January 15, 1992

Accepted April 2, 1992